Molina Puerto, J.; Valero-Gómez, A.; Bosch, F. (2022). Thermal synthesis of Pt nanoparticles on carbon paper supports. International Journal of Hydrogen Energy. 47(97):41223-41235. https://doi.org/10.1016/j.ijhydene.2022.03.151

Thermal synthesis of Pt nanoparticles on carbon paper supports

J. Molina[1,2*], A. Valero-Gómez[1], F. Bosch[1]

[1]*AIDIMME. Instituto Tecnológico Metalmecánico, Mueble, Madera, Embalaje y Afines Parque Tecnológico. Avda. Leonardo Da Vinci, 38, 46980 Paterna (València) Spain*

[2]*Departamento de Ingeniería Textil y Papelera, EPS de Alcoy, Universitat Politècnica de València, Plaza Ferrándiz y Carbonell s/n, 03801 Alcoy, Spain*

Abstract

A thermal method of synthesis and fixation of Pt nanoparticles (Pt NPs) on carbon paper is proposed in this paper. Carbon paper was coated with H_2PtCl_6 by simple immersion in an ethanol solution containing the Pt precursor. Thereafter, H_2PtCl_6 was decomposed in inert atmosphere into Pt NPs by applying a temperature of 600ºC. Formed Pt NPs were able to oxidize the surrounding carbon fiber surface. This local thermal oxidation of carbon promoted the generation of nano-roughness and Pt NPs were embedded in the carbon fiber, thus favoring their fixation on carbon paper. Pt load can be easily controlled by the number of coating processes applied. The proposed method combines the advantage of achieving small size nanoparticles (5-10 nm) with enhanced fixation of Pt NPs when compared with electrochemical synthesis. The optimal number of coatings applied was three, which produced a complete coverage of carbon paper surface (with a Pt load of 0.18 $mg \cdot cm^{-2}$).

Keywords: platinum, nanoparticles, thermal synthesis, electrocatalyst

---

* Corresponding author. Fax: +34 *960915446*; telephone: +34 *961318559*

E-mail address: jamopue@doctor.upv.es

Declarations of interest: none

1. Introduction

Pt is the most used catalytic material for hydrogen evolution reaction (HER) due its superior performance when compared with other catalytic materials [1]. H adsorption is a crucial process in the HER and adsorption of H on Pt is close to the thermoneutral state, reason why Pt is the best HER electrocatalyst. Size of nanoparticles is crucial on their catalytic activity. Smaller nanoparticles present a higher proportion of surface atoms [2], which allows obtaining materials with higher catalytic activity due to their enhanced surface area, thus improving catalyst utilization. Electronic properties of metal nanoparticles are also affected by size, and metal nanoparticles with low size (< 1 nm) would interact differently with reactants, when compared with bigger size nanoparticles [3].

Different methods have been reported for the synthesis of Pt, mainly chemical and physical [4]. Chemical reduction [5,6], electrochemical reduction [5,6] and chemical vapor deposition methods [7] are included among chemical methods of synthesis of Pt NPs. Among physical production methods, laser ablation technique [8], aerosol-assisted deposition [9], electron-beam-induced reduction [10], flame synthesis [11], sputtering [12] or plasma [13] are included. Chemical reduction methods are among the most used

methods due to its simplicity and control on the characteristics of the NPs that can be achieved by controlling precursor concentration, temperature, use of organic or inorganic ligands, etc. In the chemical methods of synthesis, a reductant is used to achieve the reduction of Pt precursors in solution. Afterwards, Pt NPs are collected and can be deposited on the surface of supporting materials to produce catalytic materials with application in energy conversion systems. For example, in the case of fuel cells and electrolyzers, Pt NPs are mixed with carbon nanoparticles and Nafion to produce a paste that can be applied on the surface of a membrane to produce a catalyst coated membrane. If this paste is applied on the surface of supporting substrates (carbon cloth, carbon paper, etc.) a catalyst coated substrate is produced [14]. This method has the drawback that Pt NPs located in the interior of the paste are less active than outer Pt NPs. Electrochemical methods of synthesis have the advantage that Pt NPs are deposited directly on the surface of the target substrate and do not need posterior processing as in the case of chemical methods of synthesis. However, the size of Pt NPs obtained by means of electrochemical methods is normally bigger than the one obtained by means of chemical methods. The typical morphology of NPs obtained by means of electrochemical methods is cauliflower-like, where Pt NPs are aggregated [6]. Carbon materials are among the most used support for Pt NPs [15] in electrochemical applications due to its conductivity, high surface area, resistance to acids and bases, etc. [16].

The present paper proposes a thermal method of synthesis of Pt NPs on carbon paper substrate. Thermal methods of synthesis of Pt NPs have not been extensively used in bibliography. These methods consist in the decomposition of a Pt salt precursor after the application of an adequate temperature [9, 17]. The thermal decomposition of H_2PtCl_6 on single crystalline silicon substrates [9]; or more complex compound bis(pyridyl)-coordinated platinum(II)-containing metallopolyyne polymer have been reported [17].

The proposed method in this paper combines simplicity (impregnation of precursor on carbon fibers and posterior thermal decomposition to produce Pt NPs) with a good fixation of the nanoparticles on the carbon paper support. The fixation of Pt NPs is achieved by the in-situ generation of nanoporosity that allows the embedment of Pt NPs into carbon fibers. In addition, Pt load can be easily controlled by the number of thermal cycles applied. With three thermal cycles of deposition, an optimal load of approximately 0.18 $mg \cdot cm^{-2}$ Pt was achieved, obtaining a complete coverage of the carbon fibers. Electrochemical characterization of the novel electrodes was benchmarked with electrodes coated electrochemically with Pt loads of 0.5 $mg \cdot cm^{-2}$ and 2 $mg \cdot cm^{-2}$.

2. Experimental

2.1. Reagents and materials

Sulfuric acid, ethanol and methanol were acquired from Merck. $H_2PtCl_6 \cdot 6H_2O$ (hexachloroplatinic acid hexahydrate) was purchased from Merck. Hydrophilic carbon paper electrodes (gas diffusion electrodes) electrodes were acquired from Freudenberg (H23).

2.2. Electrochemical synthesis of Pt NPs on carbon paper

Electrochemical synthesis of Pt NPs on carbon paper electrodes was performed in 2 mM H_2PtCl_6 / 0.5 M H_2SO_4 solution. A three-electrode configuration was used, with a strip (1 cm x 1.5 cm of exposed area which was controlled with Teflon®) of the carbon paper as the working electrode, a Pt counter electrode and an Ag/AgCl reference electrode. Electrical contact of the carbon paper was made by locating the carbon paper between

two rectangular DSA electrodes which were connected to the potentiostat-galvanostat with metallic tweezers. In this way, damage to the carbon paper by metallic tweezers was avoided. Potentiostatic synthesis at 0 V was performed during the necessary time to achieve a theoretical Pt load of 0.5 $mg \cdot cm^{-2}$ and 2 $mg \cdot cm^{-2}$ (which would be equivalent to 1 $C \cdot cm^{-2}$ and 4 $C \cdot cm^{-2}$ of electrical charge, respectively, according to Faraday's law). Electrochemical synthesis was performed in inert gas atmosphere (nitrogen) after removing oxygen by bubbling N_2 gas for 10 minutes.

2.3. Thermal synthesis of Pt nanoparticles on carbon paper

A square of carbon paper (9 x 9 cm) was immersed in a 20 mM H_2PtCl_6 in ethanol solution for 1 minute. After immersion, samples were hanged till ethanol was completely evaporated. In this way H_2PtCl_6 was deposited on carbon fibers. Thereafter, a thermal treatment was performed in a Linn High Term FRV-450/500/1000-Vac furnace at 600ºC for 2 hours to achieve the thermal decomposition of H_2PtCl_6 into Pt NPs. Thermal treatment was performed in Ar atmosphere to avoid thermal oxidation of carbon paper at this temperature. The whole process was repeated between 1 and 4 times to synthesize samples with 1, 2, 3 and 4 coatings of Pt NPs. Pt load was determined by Inductively Coupled Plasma optical emission spectrometer (ICP-OES) (PerkinElmer OPTIMA 2000™) after dissolving Pt NPs supported on carbon paper in boiling aqua regia. Concentration obtained was 0.06 $mg \cdot cm^{-2}$, 0.09 $mg \cdot cm^{-2}$, 0.18 $mg \cdot cm^{-2}$ and 0.16 $mg \cdot cm^{-2}$ for 1, 2, 3 and 4 coatings, respectively.

2.4. Field emission scanning electron microscopy (FESEM)

A Zeiss Ultra 55 field emission scanning electron microscope (FESEM) was used to observe the distribution and morphology of Pt NPs. Samples were not coated with an additional conductive coating (Pt, Au or C) since carbon paper an Pt NPs were conductive. Micrographs with secondary and backscattered electrons were obtained using an acceleration voltage of 2 kV. Backscattered electron micrographs were advantageous to observe Pt NPs distribution since their high atomic weight produced an adequate contrast with carbon paper substrate (Pt NPs appear as white zones in the micrographs).

2.5. Electrochemical measurements

Electrochemical measurements were performed with an Autolab PGSTAT302N potentiostat/galvanostat. Characterization of the different electrodes synthesized was performed with a three-electrode configuration, where the synthesized electrodes acted as the working electrode, Pt sheet was the counter electrode and Ag/AgCl reference electrode was used as potential reference. Electrochemical activity of the different synthesized electrodes was performed in 0.5 M H_2SO_4 for testing hydrogen adsorption/desorption processes and in 0.5 M H_2SO_4 / 0.5 M CH_3OH to test electrocatalytic activity for methanol oxidation. Electrochemical characterization was performed in inert gas atmosphere (nitrogen) after removing oxygen by bubbling N_2 gas for 10 minutes.

Chronoamperometry technique was used to test the stability of the optimal electrodes (3 thermal coatings applied). An initial voltammetric characterization was performed between 1 V and -0.5 V, showing hydrogen evolution reaction at potentials < 0.2 V. Two types of stability tests were performed in 0.5 M H_2SO_4 at -0.5 V, registering the variation of current density with time. In the first one, the duration of chronoamperometry test was

1 h. After the test, voltammetric characterization was also performed as a way of comparing any change in electroactivity. This process (chronoamperometry and voltammetric characterization) was repeated 5 times. In the second type of stability test, chronoamperometry was performed for 24 h.

3. Results and discussion

3.1. Electrochemical synthesis of Pt NPs on carbon paper

Carbon fibers are quite smooth and no apparent porosity can be observed (Fig. 1-a,b). Only extrusion lines on the surface of the fibers can be observed since carbon fibers are normally obtained after carbonization of polyacrylonitrile fibers. Generally, the fixation of nanoparticles on the surface of carbon fibers is challenging and sometimes is not adequate due to the lack of surface roughness. For this reason, plasma techniques have been used in bibliography for the generation of roughness and functional groups that promote anchoring of nanoparticles [18,19]. In this study, hydrophilic carbon paper has been used to favor the interaction between Pt NPS and the carbon paper. However, the interaction between Pt NPs and the carbon substrate is not sufficient and delamination of Pt can take place due to the lack of mechanical adhesion between both components. For example, this can be seen in the electrochemical synthesis of Pt NPs, where delamination of Pt deposit can take place (Fig. 1-f). In the electrochemical synthesis, a carbon paper electrode was coated with Pt NPs synthesized by means of potentiostatic synthesis. Electrosynthesis was performed at 0 V (vs. Ag/AgCl) and electrical charges of 1 $C \cdot cm^{-2}$ and 4 $C \cdot cm^{-2}$ were used, which would be equal to 0.5 $mg \cdot cm^{-2}$ and 2 $mg \cdot cm^{-2}$ of Pt NPs theoretical load, respectively. These loads were calculated considering that the only process that takes place during electrosynthesis is the reduction of $PtCl_6^{2-}$ to Pt with 100

% efficiency [20,21]. According to Faraday's law, the quantity of Pt deposited (mPt) would be [20,21]:

$$mPt = \frac{QPt \cdot M}{4 \cdot F}$$

Where QPt is the electrical charge consumed during the electrosynthesis of Pt ($C \cdot cm^{-2}$); M is 195.09 $g \cdot mol^{-1}$ corresponding to the atomic weight of Pt; 4 is the number of electrons involved in the reduction of $PtCl_6^{2-}$ to Pt and F is the Faraday constant (96845 $C \cdot mol^{-1}$). These electrodes were also electrochemically characterized and used to benchmark the electrocatalytic activity of thermally synthesized electrodes. Fig. 2 shows the chronoamperograms obtained for the two electrical charges used in the electrochemical synthesis (1 $C \cdot cm^{-2}$ and 4 $C \cdot cm^{-2}$). As can be seen, current density increases when deposition time increases. This can be related to the increase of the surface area as Pt NPs are progressively deposited on the carbon paper electrode. In the case of the higher Pt load (2 $mg \cdot cm^{-2}$), current density tends to stabilize at the end of the electrodeposition since the growth of Pt takes place on previously deposited Pt NPs (three-dimensional growth of Pt NPs). The exposed area of Pt NPs to the electrolyte stabilizes since inner NPs, which are coated with Pt NPs, do not have access to the electrolyte and cannot show their electrocatalytic activity.

Fig. 1-c,d,e,f shows the micrographs of carbon paper electrode coated with Pt NPs obtained by means of potentiostatic synthesis with a Pt load of 0.5 $mg \cdot cm^{-2}$. In this case only micrographs using secondary electrons were obtained since the presence of Pt was obvious and the whole surface of carbon fibers was coated. Electrochemical deposition is influenced by current distribution on the substrate. As can be seen in the bottom part of micrograph in Fig. 1-c, an inner fiber was not coated with Pt NPs since current flow in this fiber was not sufficient to allow Pt electrodeposition. The morphology of

electrodeposited Pt was globular as can be seen in Fig. 1-d,e, where individual nanoparticles aggregate to form cauliflower-like nanoparticles. This morphology is typical for Pt electrochemically grown [6]. In some zones, detachment of Pt deposit from the surface of carbon fiber was observed due to the lack of adhesion between both surfaces as can be seen in Fig. 1-f. Thus, electrochemical deposition allows a facile growth of Pt nanoparticles on carbon paper electrode, however adhesion is not adequate, and delamination can take place. Pt coverage on surface fibers was almost complete; however inner fibers were not properly coated due to inefficient current distribution on the carbon paper substrate.

Micrographs of fibers coated with a Pt load of 2 $mg \cdot cm^{-2}$ are not shown since the same morphology was observed. In the case of higher Pt loads, the additional growth of Pt NPs was produced in the axis perpendicular to the fiber. Once the surface of the fibers is completely coated with Pt NPs, the three-dimensional growth takes place.

3.2. Thermal synthesis of Pt NPs on carbon paper

Figure 3 shows micrographs of the carbon paper coated with H_2PtCl_6 before applying the thermal treatment. As can be seen in the micrographs, H_2PtCl_6 is deposited on the fibers in the form of crystals. This can be best observed in the micrographs with higher magnification (Fig. 3-d,e).

According to bibliography [22], $H_2PtCl_6 \cdot 6H_2O$ thermograms in N_2 atmosphere showed three weight losses, attributed to the loss of water and chlorine. Above 523ºC, remaining weight stabilizes around 40% which would be equal to weight percentage of Pt in $H_2PtCl_6 \cdot 6H_2O$. Hence the temperature of 600ºC which was the temperature applied for the synthesis of nanoparticles was sufficient to allow the thermal decomposition of the precursor and promote the formation of Pt NPs. The Ar atmosphere that was maintained

during the thermal treatment impeded the thermal oxidation of the carbon paper. However, some degree of thermal oxidation was observed during the experiments as will be explained later (a weight loss was also measured confirming the thermal oxidation).

Fig. 4 shows the micrographs of carbon paper coated with Pt NPs by means of thermal treatment. Low magnification micrographs are used in Fig. 4 to present a general view of Pt distribution. Nanoparticles obtained by means of thermal methods were smaller than the ones obtained by electrochemical methods, thus with secondary electron micrographs it was not possible to observe properly the distribution of Pt NPs. This is the reason why backscattered electrons micrographs were obtained. In Fig. 4-a, the sample coated with one thermal coating is presented. As can be seen, the carbon fibers are partially coated with Pt NPs. When 2 coatings were applied, the coverage degree increased substantially as can be seen in Fig. 4-b, although samples were not completely coated with Pt NPs. With 3 coatings, carbon fibers were completely coated with Pt nanoparticles as can be seen in Fig. 4-c, where carbon fibers appear whitish due to the presence of Pt NPs. With 4 coatings no substantial changes were observed under this magnification and a complete coverage of the fibers by Pt NPs was observed (Fig. 4-d).

Figure 5 shows high magnification micrographs (x100000) of the different carbon paper electrodes. Micrographs at this magnification were also obtained by backscattered electrons to observe the distribution of Pt NPs. With 1 thermal coating, partial coverage of the carbon surface was observed (Fig. 5-a). With 2 coatings, the coating degree was substantially increased (Fig. 5-b). With three coatings, the surface was completely coated with Pt NPs (Fig. 5-c). With 1, 2 and 3 coatings the nanoparticle size was not substantially modified. However, with 4 coatings a substantial increase of nanoparticle was observed (Fig. 5-d). The increase of nanoparticle size is detrimental since effective catalyst area decreases with the increase of nanoparticle size. Considering the information obtained

from the micrographs, three thermal coatings would be the optimal to apply. The application of a higher number of coatings increased the Pt content; however, an increase of NPs size also took place.

Figure 6 shows secondary electron micrographs of the carbon paper coated with Pt NPs obtained by thermal methods. With secondary electrons, morphology of nanoparticles and carbon can be better appreciated. With 1 coating process, the coating degree was not sufficient and only some nanoparticles were observed on the surface of the fibers (Fig. 6-a). With 2 coatings, the formation of Pt NPs of low size (5-10 nm) could be observed on the surface of carbon paper (Fig. 6-b). The distribution was homogeneous; however, the coating degree of the surface was not complete. With 3 coatings the surface was completely coated with Pt NPs (Fig. 6-c). A slight increase of nanoparticles size was also observed. With 4 coatings, the most remarkable fact was the increase of nanoparticles size as can be seen in Fig. 6-d; where nanoparticles of 50-70 nm could be observed. Although the fusion temperature of Pt nanoparticles is lower than bulk metal (~1768 ºC) [23], at the temperature of synthesis of 600ºC Pt NPs are not expected to fuse together. Hence, the increase of NPs size is produced during the repeated thermal synthesis process, increasing progressively the diameter of NPs.

Therefore, with 3 thermal coating processes, a proper distribution of Pt NPs and with small size was obtained. A higher number of coatings produced an increase of nanoparticle size which would be detrimental for electrocatalytic activity.

If compared with Fig. 1-a,b, where micrographs of carbon paper are presented, an increase of the roughness of carbon fibers can be clearly appreciated in all micrographs presented in Fig. 6. This roughness helps to anchor Pt NPs on carbon surface by providing a physical interaction of Pt NPs with carbon fibers. Since this roughness was not originally present on the surface of the fibers, it should be created during the thermal treatment applied for

the synthesis of Pt NPs. The process of roughness creation can be better appreciated in Fig. 6-d, where nanoparticles are bigger. As can be seen, nanopores are created in the zone where Pt NPs are formed. The creation of the nanopores can be attributed to the local thermal oxidation of the carbon support. This phenomenon has been previously observed in bibliography on Pt/carbon catalysts in proton exchange membrane fuel cells [24-25] (at operating temperatures below 200ºC) and was detrimental for its performance. The loss of activity was attributed to the release of catalytic particles arising from the loss of supporting carbon, or the emitted gases can poison Pt NPs [24]. The presence of Pt accelerates the thermal oxidation of the carbon support and thermal oxidation of carbon support is produced at lower temperatures than without the presence of Pt [26-28]. Thermal oxidation increases with the quantity of Pt present as well as with the temperature [24]. It has also been reported that in inert atmosphere, Pt NPs are able to oxidize the surface of carbon fibers in the zone of contact between Pt NPs and carbon substrate [24]. The loss of carbon which would be detrimental for the performance is taken as an advantage in the synthesis and fixation of Pt NPs in the study reported in the present paper. Guterman et al. [27] proposed a mechanism where Pt NPs moved deeper into the carbon as thermal oxidation proceeded in oxygen containing atmosphere. This has been clearly observed in the present paper, where a progressive oxidation of the carbon support produces the embedment of Pt NPs inside the carbon support. It is expected that Pt load and NPs size could be also controlled by means of adjusting the concentration of the precursor used to coat the carbon paper, so this possibility could be explored in future studies.

The thermal oxidation of the carbon paper can be produced through oxygen containing functional groups of the carbon paper [24]. In the interface between Pt and carbon fibers, the decomposition of oxidized species takes place, producing the oxidation of carbon

support to CO_2. Without the presence of a catalyst and in inert atmosphere, the less thermally stable functional groups on carbon surface are carboxylic groups [26]. Other functional groups such as carbonyl, ether or quinine are stable in inert atmosphere till temperatures above 700ºC [26]. However, the presence of Pt as a catalyst is expected to reduce the thermal stability of these functional groups. In the present study, a hydrophilic carbon paper was used; hence oxygen-containing functional groups are present on carbon fibers. Other proposed route for thermal oxidation of carbon in inert atmosphere is the thermal decomposition of Pt surface oxides which produce O_2 that oxidizes carbon surface [24].

Fig. 7 shows the EDX characterization of the different substrates. In the case of carbon paper, only C and O are present in the composition of the carbon paper (Fig. 7-a). When H_2PtCl_6 was deposited on the surface of carbon paper (Fig. 7-c), Pt and Cl appeared in the spectrum. When applying the thermal treatment, H_2PtCl_6 decomposed into Pt and Cl disappeared of the spectrum (Fig. 7-c). In the case of electrochemically synthesized Pt, Cl was also not present due to electrochemical reduction of H_2PtCl_6 to Pt NPs (Fig. 7-d).

3.3. Electrochemical characterization

Electrochemical characterization was performed to test the electroactivity of the synthesized electrodes. Fig. 8 shows the characterization of the different electrodes by cyclic voltammetry in 0.5 M H_2SO_4, where hydrogen adsorption/desorption processes can be observed between -0.2 V and 0.1 V. As can be seen, bare carbon paper showed no activity towards hydrogen/adsorption processes (dotted black line) in the potential range studied. All the samples containing Pt showed the appearance of characteristic adsorption/desorption processes of hydrogen [29]. As can be seen in the graph, there was an increase of electrochemical activity with the number of thermal processes applied till

3 coatings. When 4 coatings were applied, currents obtained decreased, despite having a higher Pt content. This effect can be attributed to the increase of nanoparticle size as could be previously observed in FESEM characterization. Electrochemical characterization of the two paper electrodes coated electrochemically with Pt (0.5 $mg \cdot cm^{-2}$ and 2 $mg \cdot cm^{-2}$) is also presented for comparison. As can be seen in the voltammograms, electrical charge is higher for the higher Pt load of 2 $mg \cdot cm^{-2}$ if compared with the 0.5 $mg \cdot cm^{-2}$ one. However, when compared with thermally synthesized electrodes, electrochemically synthesized samples only surpass the sample coated with 1 thermal cycle, which had a very low Pt content as observed by FESEM characterization. When 4 coatings were applied a decrease of electroactivity was observed due to the increase of Pt NPs size, although catalytic activity is still higher than the obtained for electrochemically synthesized samples.

Table 1 shows the results of hydrogen adsorption charge (calculated with the integration of the hydrogen adsorption area in the voltammogram obtained in 0.5 M H_2SO_4); electrochemical surface area (ECSA) (calculated dividing the hydrogen adsorption charge by the Pt loading and the theoretical value for the adsorption of a hydrogen monolayer on Pt surface (210 $\mu C \cdot cm^{-2}$) and roughness factor (calculated dividing the normalized hydrogen adsorption charge ($\mu C \cdot cm^{-2}$) by the theoretical value for the adsorption of a hydrogen monolayer on Pt surface (210 $\mu C \cdot cm^{-2}$) [30] for the different samples. Comparing the results of surface area, thermal method of synthesis showed better results than the electrochemical one. Highest surface area was obtained for 2 and 3 Pt coatings thermally applied, with similar values (~30 m^2/g). This indicates a similar size of Pt NPs as observed by FESEM. However, if roughness factor is compared for both samples, it was the double in the case of the sample with 3 coatings. This indicates a better coverage of the surface of the carbon paper by Pt NPs as observed by FESEM previously. Results

reported in bibliography for ECSA range from 3.64 m^2/g for pencil graphite electrodes electrochemically coated with Pt NPs [31] to 108 m^2/g for Pt/C paste electrodes [32]. The ECSA reported in our study is similar to other papers where graphene materials and carbon nanotubes are employed [33], being the proposed method of synthesis proposed in our study, easier.

Figure 9 shows the voltammetric characterization in 0.5 M methanol/ 0.5 M H_2SO_4 solution to test the electrocatalytic properties of the different electrodes towards methanol oxidation. Methanol oxidation reaction was selected to test electroactivity since this reaction takes place on the anode in fuel cells [34]. As can be seen, carbon paper substrate has no catalytic activity since no oxidation peaks appear in the corresponding voltammogram. When Pt was deposited on the carbon paper, two oxidation peaks could be clearly observed in the different voltammograms. The peak at higher potential is produced in the forward scan and is due to the oxidation of freshly chemisorbed species arising from methanol adsorption. The second oxidation peak that appears in the backward scan at lower potentials is due to the oxidation of carbonaceous species not completely oxidized in the forward scan [30, 35]. When 1 thermal coating was applied on Pt, electroactivity towards methanol oxidation increased slightly, with an oxidation current density of 0.73 $mA \cdot cm^{-2}$. With 2 thermal coatings, the current density increased till 5.16 $mA \cdot cm^{-2}$. With 3 thermal coatings the current density continued to increase till 8.97 $mA \cdot cm^{-2}$ which was the maximum current density achieved in this study. However, when 4 thermal coatings were applied, the current density decreased till 4.19 $mA \cdot cm^{-2}$. In the case of electrochemically synthesized Pt coatings, the current achieved was 4.54 $mA \cdot cm^{-2}$ and 2.3 $mA \cdot cm^{-2}$ for a Pt load of 2 $mg \cdot cm^{-2}$ and 0.5 $mg \cdot cm^{-2}$, respectively.

In table 2, the specific activity for methanol oxidation for the optimal electrode developed in this paper is compared with other methods of synthesis of Pt-based catalysts reported

in bibliography. As can be seen, higher specific activity is obtained with the thermal method of synthesis proposed in this paper.

The results obtained for methanol oxidation follow a similar trend to the one obtained for characterization in 0.5 M H_2SO_4, confirming that the highest catalytic activity was achieved with 3 thermal coatings. An additional increase of Pt load produced an increase of Pt NPs size and consequently electroactivity decreased despite having a higher Pt load with 4 thermal coatings. Thermal coatings also produced a higher catalytic activity than electrochemically synthesized coatings. This can be attributed to the smaller size of Pt NPs obtained in the case of thermal synthesis. In addition, with thermal coatings a lower Pt load was applied on the carbon paper, thus maximizing the exposed area of Pt. With electrochemical synthesis, the surface of carbon fibers is firstly coated with Pt NPs, and then a three-dimensional growth of Pt NPs takes place. The increase of Pt load in electrochemical synthesis is not effective since inner nanoparticles cannot act due to the fact that outer nanoparticles hinder the diffusion of the electrolyte till inner nanoparticles; thus, inner electrocatalyst is not active. With the thermal synthesis, an excellent dispersion of Pt NPs was achieved. In addition, the small size of Pt NPs maximized the catalytic area, thus obtaining better electrocatalytic materials. However, if the quantity of Pt applied is excessive, the NPs size increases and the catalytic area decreases.

Stability of the electrodes obtained by the optimal method of synthesis (3 thermal coatings) was tested by chronoamperometry tests. An initial voltammetric characterization (Figure 10), performed between 1 V and -0.5 V, showed that at potentials < 0.2 V, hydrogen evolution reaction was observed. Current densities achieved at -0.5 V were around 30 $mA \cdot cm^{-2}$, so this potential was selected to carry out stability tests of the electrodes for hydrogen evolution reaction. The electrochemical response of the carbon

paper is also compared in the same figure, showing less catalytic activity and higher overpotential for hydrogen evolution reaction.

The first chronoamperometry test was carried out in 0.5 M H_2SO_4 at -0.5 V during 1 h and 5 consecutive cycles were performed (Figure 11). After each of the cycles, a voltammetic characterization was also performed to test any change in the electroactivity. In the five consecutive chronoamperometry tests carried out, current density was constant for 1 h in each of the five cycles, with a value of current density around 30 $mA \cdot cm^2$. The voltammetric characterization performed after each chronoamperometry test also showed no significant change in the voltammetric response. In Figure 10, initial voltammetric characterization and after 5 cycles of chronoamperometry are compared, showing no meaningful differences. Chronoamperometry tests and cyclic voltammetry characterization point out the stability of the developed electrodes for hydrogen evolution reaction.

The second type of stability test was performed during 24 h by chronoamperometry at -0.5 V in 0.5 M H_2SO_4. This test also showed the stability of the developed material in continuous operation at -0.5 V (Figure 12), where no significant variation of the current density was observed. The initial current density was -31.3 $mA \cdot cm^{-2}$ and after 24 h was 31.0 $mA \cdot cm^{-2}$. Voltammetric characterization of the electrode after the test not only not showed loss of electroactivity but an increased electroactivity in the hydrogen desorption region was observed (Fig. 10).

The method developed in this paper is simple and has the advantage of obtaining a good fixation on carbon paper due to the in-situ generation of nanoporosity. The synthesized electrodes could be applied in electrocatalysis (PEM electrolyzers, fuel cells, etc.).

4. Conclusions

A novel method for the synthesis of Pt NPs-on carbon paper supports is presented in this paper. Pt NPs-are formed on carbon paper substrates by thermal decomposition of the Pt precursor (H_2PtCl_6) that has been previously deposited on the surface of carbon paper. The decomposition of Pt precursor is performed at 600ºC in inert atmosphere to avoid thermal oxidation of the carbon support. Despite using inert atmosphere, Pt NPs promote the local oxidation of the carbon support in the interfacial zones between Pt NPs and the carbon paper, thus creating nanoporosity on the carbon supports. An oxygen source is needed to produce local carbon oxidation, which are the functional groups of carbon fibers. The result is that Pt NPs are formed on carbon support and are embedded in carbon support due to the thermal oxidation in the interface between Pt NPs and carbon fibers. The created nanoporosity facilitates the adhesion of Pt NPs on carbon paper if compared with electrochemical methods of synthesis. The thermal deposition of Pt deposition favors the creation of NPs with small size (5-10 nm) with an excellent distribution over all the fibers that compose the carbon paper. Pt load can be easily controlled by the number of deposition cycles applied. With the concentration of precursor used in this paper, the application of 3 coating cycles produced the optimal results (Pt load of 0.18 $mg \cdot cm^{-2}$). A higher number of coating cycles produced an increase of NPs size which was detrimental for electrocatalytic activity.

Electrochemical characterization of synthesized electrodes has been performed towards hydrogen adsorption/desorption processes as well as methanol oxidation. Thermally coated carbon paper with Pt NPs showed higher electroactivity than the ones electrochemically synthesized, despite having a lower Pt load (~0.18 $mg \cdot cm^{-2}$ vs. 0.5 $mg \cdot cm^{-2}$ / 2 $mg \cdot cm^{-2}$). The best performance of the thermally synthesized electrodes can be attributed to the smaller size and optimal dispersion of Pt NPs achieved with thermal

synthesis. Electrodes obtained by the optimal method of deposition (3 thermal coatings) also showed good performance and stability for hydrogen evolution reaction at -0.5 V in continuous and discontinuous operation.

Acknowledgements

This work was supported by the Instituto Valenciano de Competitividad Empresarial (IVACE) (project references IMDECA/2016/50, IMDEEA/2017/116, IMDEEA/2018/26) and European Union (FEDER). Electron Microscopy Service of the UPV (Universitat Politècnica de València) is gratefully acknowledged for help with FESEM and EDX characterization.

Role of the funding source

The funding source had no involvement in study design; in the collection, analysis and interpretation of data; in the writing of the report; and in the decision to submit the article for publication.

References:

[1] A. Eftekhari. Electrocatalysts for hydrogen evolution reaction. Int. J. Hydrogen Energ. 42 (2017) 11053–11077.

[2] K.J. Klabunde, J.Stark, O. Koper, C. Mohs, D.G. Park, S. Decker, Y. Jiang, I. Lagadic, D. Zhang. Nanocrystals as Stoichiometric Reagents with Unique Surface Chemistry. J. Phys. Chem. 100 (1996) 12142–12153.

[3] L. Liu, A. Corma. Metal Catalysts for Heterogeneous Catalysis: From Single Atoms to Nanoclusters and Nanoparticles. Chem. Rev. 118 (2018) 4981–5079.

[4] D. Pedone, M. Moglianetti, E. De Luca, G. Bardi, P.P. Pompa. Platinum nanoparticles in nanobiomedicine. Chem. Soc. Rev. 46 (2017) 4951–4975.

[5] C.R.K. Rao, D.C. Trivedi. Chemical and electrochemical depositions of platinum group metals and their applications. Coordin. Chem. Rev. 249 (2005) 613–631.

[6] S. E. Stanca, F. Hänschke, A. Ihring, G. Zieger, J. Dellith, E. Kessler, H.-G. Meyer. Chemical and Electrochemical Synthesis of Platinum Black. Sci. Rep. 7 (2017) 1074.

[7] H. Kim, S.H. Moon. Chemical vapor deposition of highly dispersed Pt nanoparticles on multi-walled carbon nanotubes for use as fuel-cell electrodes. Carbon 49 (2011) 1491–1501.

[8] M. Cueto, M. Sanz, M. Oujja, F. Gámez, B. Martínez-Haya, M. Castillejo. Platinum Nanoparticles Prepared by Laser Ablation in Aqueous Solutions: Fabrication and Application to Laser Desorption Ionization. J. Phys. Chem. C 115 (2011) 22217–22224.

[9] O. Paschos, P. Choi, H. Efstathiadis, P. Haldar. Synthesis of platinum nanoparticles by aerosol assisted deposition method. Thin Solid Films 516 (2008) 3796–3801.

[10] E.U. Donev, J.T. Hastings. Electron-Beam-Induced Deposition of Platinum from a Liquid Precursor. Nano Letters 9 (2009) 2715–2718.

[11] R. Strobel, S.E. Pratsinis. Flame Synthesis of Supported Platinum Group Metals for Catalysis and Sensors. Platinum Metals Rev. 53 (2009) 11–20.

[12] N. Soin, S.S. Roy, L. Karlsson, J.A. McLaughlin. Sputter deposition of highly dispersed platinum nanoparticles on carbon nanotube arrays for fuel cell electrode material. Diam. Relat. Mater. 19 (2010) 595–598.

[13] I.G. Koo, M.S. Lee, J.H. Shim, J.H. Ahn, W.M. Lee. Platinum nanoparticles prepared by a plasma-chemical reduction method. J. Mater. Chem. 15 (2005) 4125–4128.

[14] B. Bladergroen, H. Su, S. Pasupathi, V. Linkov Overview of Membrane Electrode Assembly Preparation Methods for Solid Polymer Electrolyte Electrolyzer. In book: Electrolysis, Edition: First, Chapter: 3, Publisher: InTech, Editors: Vladimir Linkov.

[15] S. Samad, K.S. Loh, W.Y. Wong, T.K. Lee, J. Sunarso, S.T. Chong, W.R.W. Daud. Carbon and non-carbon support materials for platinum-based catalysts in fuel cells. Int. J. Hydrogen Energ. 43 (2018) 7823–7854.

[16] Z.A.C. Ramli, S.K. Kamarudin. Platinum-Based Catalysts on Various Carbon Supports and Conducting Polymers for Direct Methanol Fuel Cell Applications: a Review. Nanoscale Res. Lett. 13 (2018) 410.

[17] P.-Y. Ho, S.-C. Yiu, D.Y. Wu, C.-L. Ho, W.-Y. Wong. One-step synthesis of platinum nanoparticles by pyrolysis of a polyplatinyne polymer. J. Organomet. Chem. 849-850 (2017) 4–9.

[18] S. Tiwari, J. Bijwe. Surface Treatment of Carbon Fibers - A Review. Proc. Tech. 14 (2014) 505–512.

[19] S.J. Park, L.Y. Meng. (2015) Surface Treatment and Sizing of Carbon Fibers. In: Carbon Fibers. Springer Series in Materials Science, vol 210. Springer, Dordrecht.

[20] J. Molina, J. Fernández, A.I. del Río, J. Bonastre, F. Cases. Characterization of azo dyes on Pt and Pt/polyaniline/dispersed Pt electrodes. Appl. Surf. Sci. 258 (2012) 6246–6256.

[21] S. Dominguez-Dominguez, J. Arias-Pardilla, A. Berenguer-Murcia, E. Morallon, D. Cazorla-Amoros, Electrochemical deposition of platinum nanoparticles on different carbon supports and conducting polymers. J. Appl. Electrochem. 38 (2008) 259–268.

[22] N.K. Sahu, A. Prakash, D. Bahadur. Role of different platinum precursors on formation and reaction mechanism of FePt nanoparticles and their electrocatalytic performance towards methanol oxidation. Dalton Trans. 43 (2014) 4892–4900.

[23] G. Guisbiers, G. Abudukelimu, D. Hourlier. Size-dependent catalytic and melting properties of platinum-palladium nanoparticles. Nanoscale Res. Lett. 6 (2011) 396.

[24] R. Sellin, J.-M. Clacens, C. Coutanceau. A thermogravimetric analysis/mass spectroscopy study of the thermal and chemical stability of carbon in the Pt/C catalytic system. Carbon 48 (2010) 2244–2254.

[25] D.A. Stevens, J.R. Dahn. Thermal degradation of the support in carbon-supported platinum electrocatalysts for PEM fuel cells. Carbon 43 (2005) 179–188.

[26] O.A. Baturina, S.R. Aubuchon, K.J. Wynne. Thermal Stability in Air of Pt/C Catalysts and PEM Fuel Cell Catalyst Layers. Chem. Mater. 18 (2006) 1498–1504.

[27] V.E. Guterman, S.V. Belenov, V.V. Krikov, L.L.Vysochina, W. Yohannes, N.Y. Tabachkova, E.N. Balakshina. Reasons for the Differences in the Kinetics of Thermal Oxidation of the Support in Pt/C Electrocatalysts. J. Phys. Chem. C 118 (2014) 23835–23844.

[28] R. Sellin, C. Grolleau, S. Arrii-Clacens, S. Pronier, J.-M. Clacens, C. Coutanceau, J.-M. Léger. Effects of Temperature and Atmosphere on Carbon-Supported Platinum Fuel Cell Catalysts. J. Phys. Chem. C 113 (2009) 21735–21744.

[29] A. Sepúlveda-Escribano, F. Coloma, F. Rodríguez-Reinoso. Platinum catalysts supported on carbon blacks with different surface chemical properties. Appl. Catal. A-Gen. 173 (1998) 247–257.

[30] J. Molina, J. Fernández, A.I. del Río, J. Bonastre, F. Cases. Synthesis of Pt nanoparticles on electrochemically reduced graphene oxide by potentiostatic and alternate current methods. Mater. Charact. 89 (2014) 56–68.

[31] L.C. Balint, I. Hulka, A. Kellenberger. Pencil Graphite Electrodes Decorated with Platinum Nanoparticles as Efficient Electrocatalysts for Hydrogen Evolution Reaction. Materials 15 (2022) 73.

[32] J.M.M. Tengco, B.A.T. Mehrabadi, Y. Zhang, A. Wongkaew, J.R. Regalbuta, J.W. Weidner, J.R. Monnier. Synthesis and Electrochemical Evaluation of Carbon Supported Pt-Co Bimetallic Catalysts Prepared by Electroless Deposition and Modified Charge Enhanced Dry Impregnation. Catalysts 6 (2016) 83.

[33] Y. Li, W. Gao, L. Ci, C. Wang, P.M. Ajayan. Catalytic performance of Pt nanoparticles on reduced graphene oxide for methanol electro-oxidation. Carbon 48 (2010) 1124–1130.

[34] A. Ashok, A. Kumar, A. Yuda, A.A. Ashraf. Highly efficient methanol oxidation reaction on durable Co_9S_8 @N, S-doped CNT catalyst for methanol fuel cell Applications. Int. J. Hydrog. Energy 47 (2022) 3346–3357.

[35] Singh RN, Awasthi R, Tiwari SK. Electro-catalytic activities of binary nano-composites of Pt and nano- carbon/multiwall carbon nanotube for methanol electro-oxidation. Open Catal. J. 3 (2010) 50–57.

[36] Q. Zhang, F. Yue, L. Xu, C. Yao, R.D. Priestley, S. Hou. Paper-based porous graphene/single-walled carbon nanotubes supported Pt nanoparticles as freestanding catalyst for electro-oxidation of methanol. Appl. Catal. B: Environ. 257 (2019) 117886.

[37] I. Carrillo, T.J. Leo, O. Santiago, F. Acción, E. Moreno-Gordaliza, M.A. Raso. Polypyrrole and platinum deposited onto carbon substrate to enhance direct methanol fuel cell electrodes behaviour. Int. J. Hydrog. Energy 43 (2018) 16913-16921.

[38] J. Byun, S.H. Ahn, J.J. Kim. Self-terminated electrodeposition of platinum on titanium nitride for methanol oxidation reaction in acidic electrolyte. Int. J. Hydrog. Energy 45 (2020) 9603-9611.

[39] S. Liu, F. Dong, Z. Tang, Q. Wang. The formation of wrapping type Pt-Ni alloy on three-dimensional carbon nanosheet for electrocatalytic oxidation of methanol. Int. J. Hydrog. Energy 46 (2021) 15431-15441.

[40] A. Papaderakis, O. Spyridou, N. Karanasios, A. Touni, A. Banti, N. Dimitrova, S. Armyanov, E. Valova, J. Georgieva, S. Sotiropoulos. The Effect of Carbon Content on Methanol Oxidation and Photo-Oxidation at Pt-TiO_2-C Electrodes. Catalysts 10 (2020) 248.

Figure captions

Figure 1. a), b) FESEM micrographs of a single strand of carbon fiber that make up the carbon paper electrode substrate. c), d), e), f) FESEM micrographs of carbon paper electrode substrate coated with Pt NPs synthesized electrochemically: (c) x 200, (d) x 5000, (e) x 50000, (f) x 20000. Electrochemical synthesis performed at 0 V (vs. Ag/AgCl) in 2 mM H_2PtCl_6 / 0.5 M H_2SO_4 with 1 $C \cdot cm^{-2}$ of electrical charge (0.5 $mg \cdot cm^{-2}$ Pt theoretical load, according to Faraday's law).

Figure 2. Chronoamperogram corresponding to the potentiostatic synthesis of Pt NPs performed at 0 V (vs. Ag/AgCl) in 2 mM H_2PtCl_6 / 0.5 M H_2SO_4 aqueous solution with 1 $C \cdot cm^{-2}$ and 4 $C \cdot cm^{-2}$ of electrical charge (0.5 $mg \cdot cm^{-2}$ and 2 $mg \cdot cm^{-2}$ Pt theoretical load, according to Faraday's law).

Figure 3. FESEM micrographs of carbon paper coated with H_2PtCl_6 before applying the thermal treatment. a) x2000, b) x5000, c) x10000, d) x20000, e) x50000, f) x50000.

Figure 4. FESEM micrographs of carbon paper coated with Pt NPs synthesized thermally by applying different number of coating processes: (a) 1 coating, (b) 2 coatings, (c) 3 coatings, (d) 4 coatings. x 500 magnification for all micrographs, backscattered electron micrographs.

Figure 5. FESEM micrographs of carbon paper coated with Pt NPs synthesized thermally by applying different number of coating processes: (a) 1 coating, (b) 2 coatings, (c) 3

coatings, (d) 4 coatings. x 100000 magnification for all micrographs, backscattered electron micrographs.

Figure 6. FESEM micrographs of carbon paper coated with Pt NPs synthesized thermally by applying different number of coating processes: (a) 1 coating, (b) 2 coatings, (c) 3 coatings, (d) 4 coatings. x 100000 for all micrographs, secondary electron micrographs.

Figure 7. EDX and FESEM characterization of: a) carbon paper, b) carbon paper + H_2PtCl_6, c) carbon paper + Pt thermally synthesized, d) carbon paper + Pt electrochemically synthesized.

Figure 8. Cyclic voltammograms of carbon paper, carbon paper + Pt NPs synthesized electrochemically (0.5 and 2 $mg \cdot cm^{-2}$ of Pt), carbon paper + Pt NPs synthesized thermally (1, 2, 3 and 4 coatings applied). 0.5 M H_2SO_4 aqueous medium, scan rate 50 $mV \cdot s^{-1}$.

Figure 9. Cyclic voltammograms of carbon paper, carbon paper + Pt NPs synthesized electrochemically (0.5 and 2 $mg \cdot cm^{-2}$ of Pt), carbon paper + Pt NPs synthesized thermally (1, 2, 3 and 4 coatings applied). 0.5 M H_2SO_4 / 0.5 M methanol aqueous medium, scan rate 50 $mV \cdot s^{-1}$.

Figure 10. Cyclic voltammograms of carbon paper and carbon paper + Pt NPs synthesized thermally (3 coatings applied) initially and after applying 5 chronoamperometry tests of 1h and after performing 1 chronoamperometry test of 24 h. 0.5 M H_2SO_4 aqueous medium, scan rate 50 $mV \cdot s^{-1}$.

Figure 11. Chronoamperometry tests (1 to 5) for carbon paper + Pt NPs synthesized thermally (3 coatings applied). -0.5 V for 3600 s in 0.5 M H_2SO_4.

Figure 12. Chronoamperometry test for carbon paper + Pt NPs synthesized thermally (3 coatings applied). -0.5 V for 24 h in 0.5 M H_2SO_4.

Table captions

Table 1. Hydrogen adsorption charge, ECSA and roughness factor for the different samples synthesized.

Table 2. Comparison of specific activity ($mA \cdot cm^{-2}$) for methanol oxidation with other Pt-based catalysts reported in bibliography.

Table 1. Hydrogen adsorption charge, ECSA and roughness factor for the different samples synthesized.

Sample	Hydrogen adsorption charge ($mC \cdot cm^{-2}$)	ECSA (m^2/g)	Roughness factor
Electrosynthesis (0.5 mg/cm^2)	4,29	4,08	20,42
Electrosynthesis (2 mg/cm^2)	5,14	1,22	24,45
Thermal synthesis (1 coating)	1,87	14,81	8,89
Thermal synthesis (2 coatings)	5,82	30,81	27,73
Thermal synthesis (3 coatings)	11,62	30,74	55,33
Thermal synthesis (4 coatings)	6,03	17,94	28,70

Table 2. Comparison of specific activity ($mA \cdot cm^{-2}$) for methanol oxidation with other Pt-based catalysts reported in bibliography.

Reference	Material	Method of synthesis	Medium	Specific activity ($mA \cdot cm^{-2}$)
[36]	Paper-based porous graphene/single-walled carbon nanotubes supported Pt NPs	Templated synthesis + electrodeposition	1 M methanol + 0.5 M H_2SO_4	1.45
[37]	Polypyrrole + Pt on carbon paper	Electron beam evaporation	1 M methanol + 0.5 M H_2SO_4	7.96
[38]	Pt-decorated TiN	Electrodeposition	0.5 M H_2SO_4 + 0.5 M $HClO_4$	0.7
[39]	Carbon nanosheets + Pt	Chemical synthesis	1 M methanol + 0.5 M H_2SO_4	4.97
[40]	Pt-TiO_2-C	Photodeposition	0.5 M methanol + 0.1 M $HClO_4$	0.8
This paper	Carbon paper + Pt NPs	Thermal synthesis	0.5 M methanol + 0.5 M H_2SO_4	8.97

Figure 1

Click here to access/download;Figure;Figure 1.tif

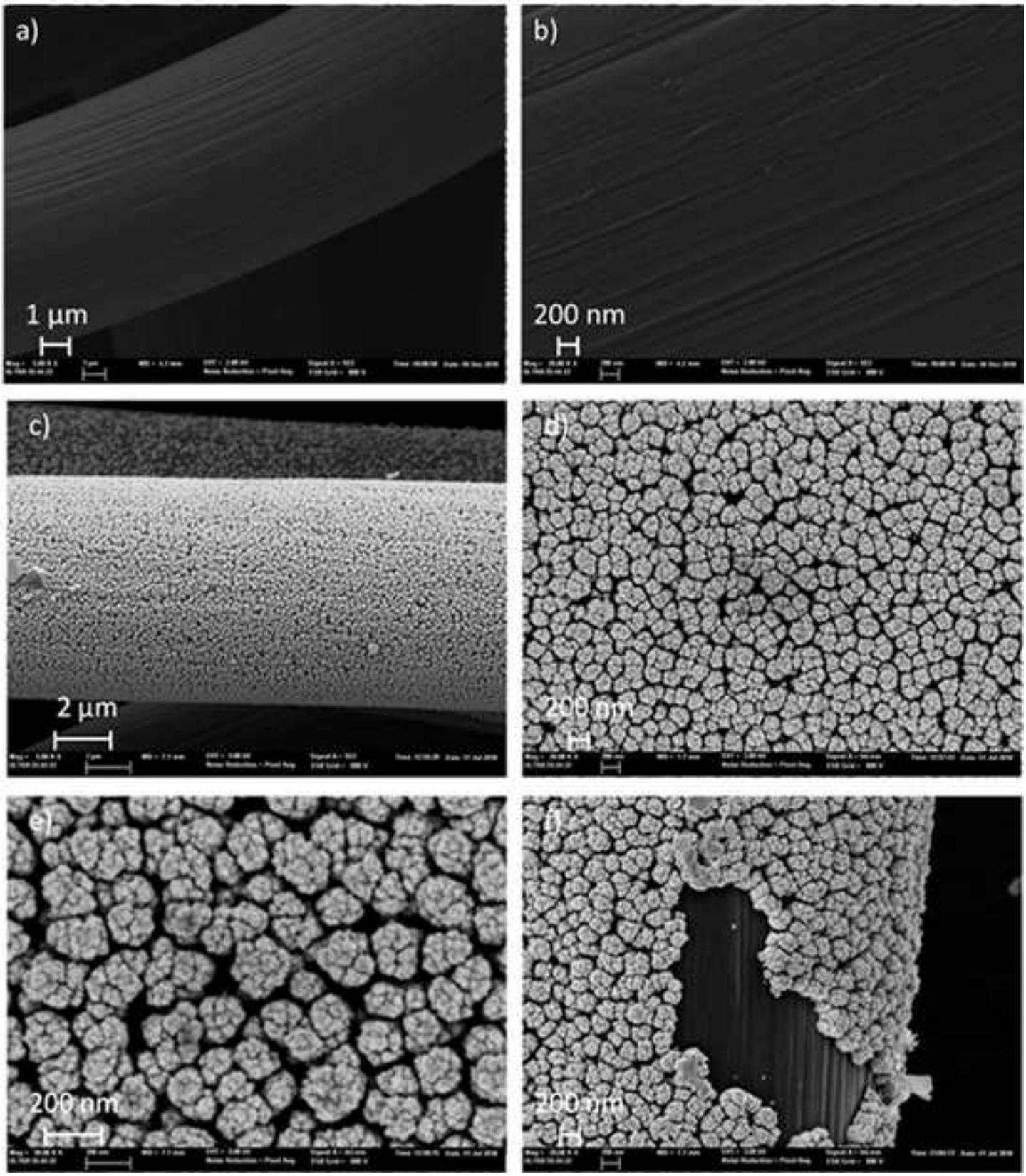

Figure 2

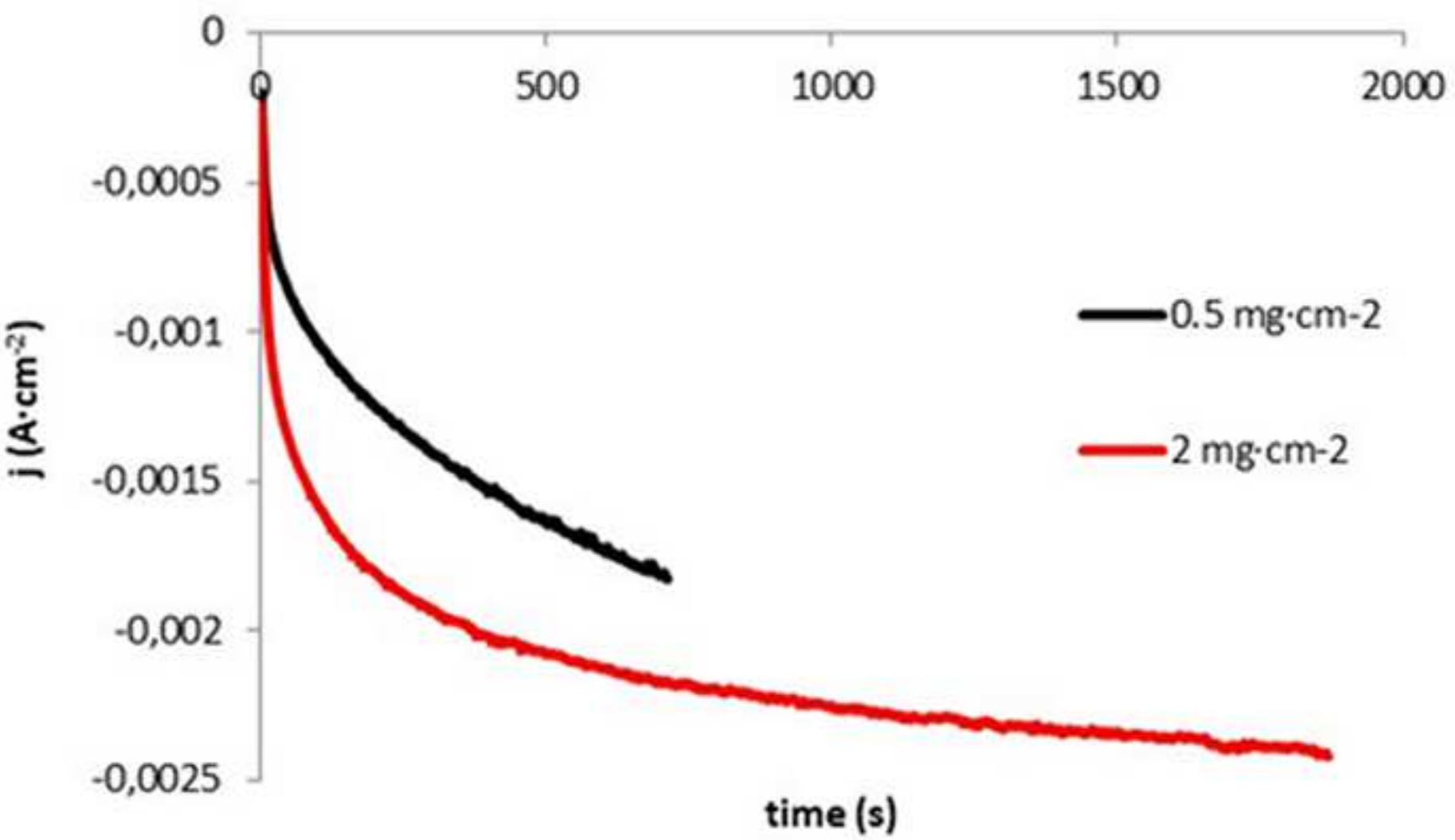

Figure 3

Click here to access/download;Figure;Figure 3.tif

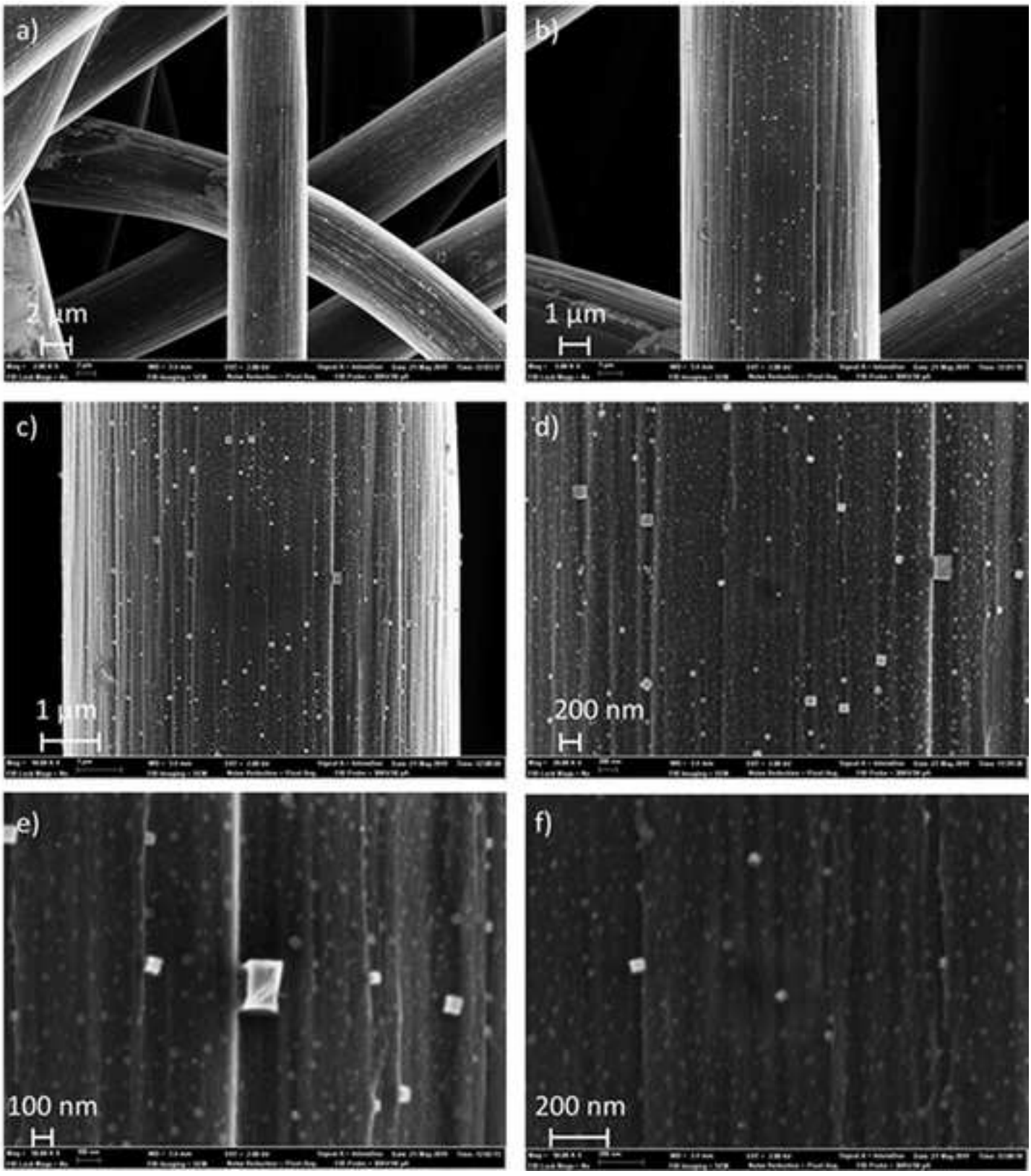

Figure 4

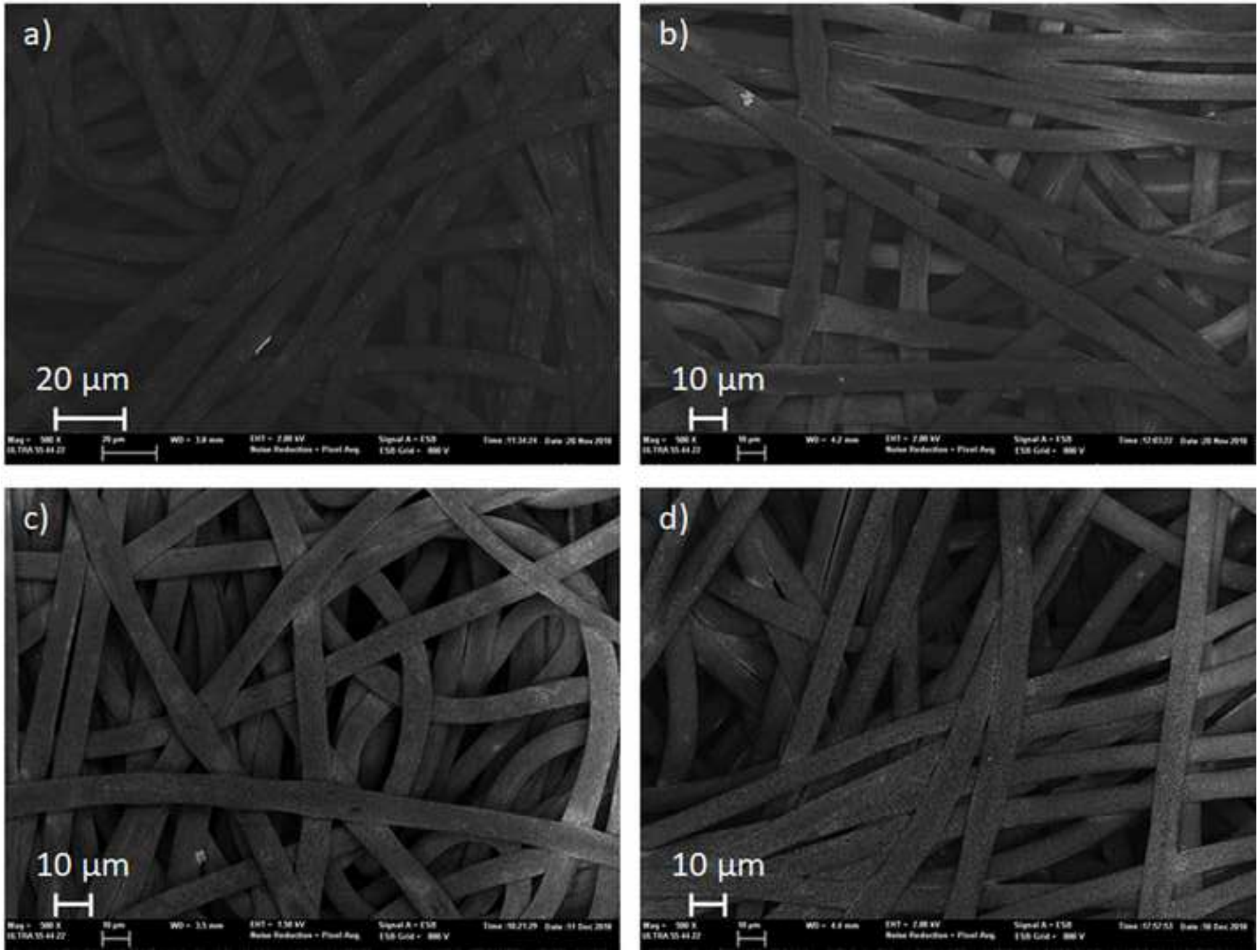

Figure 5

Click here to access/download;Figure;Figure 5.tif

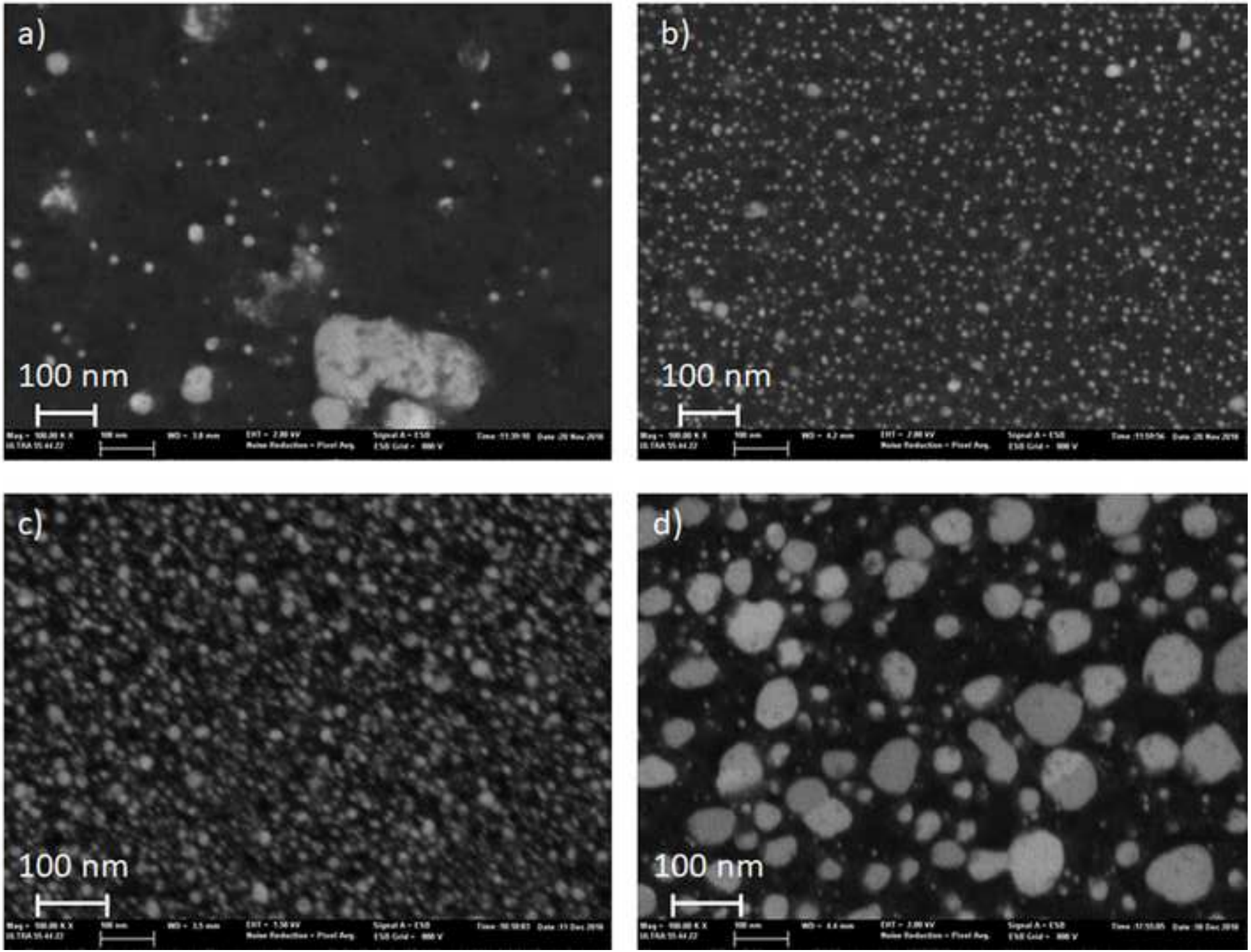

Figure 6

Click here to access/download;Figure;Figure 6.tif

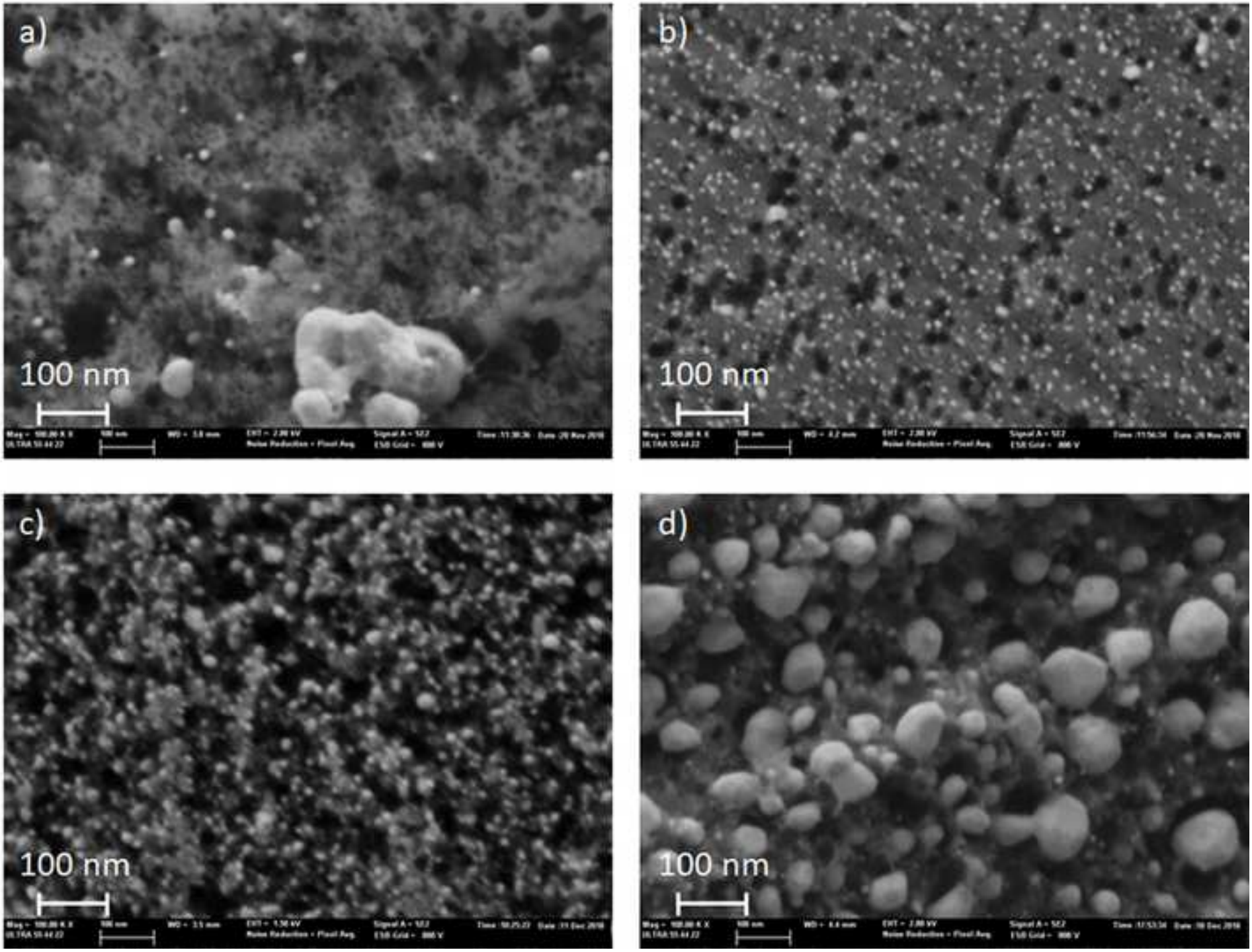

Figure 7

Click here to access/download;Figure;Figure 7.tif

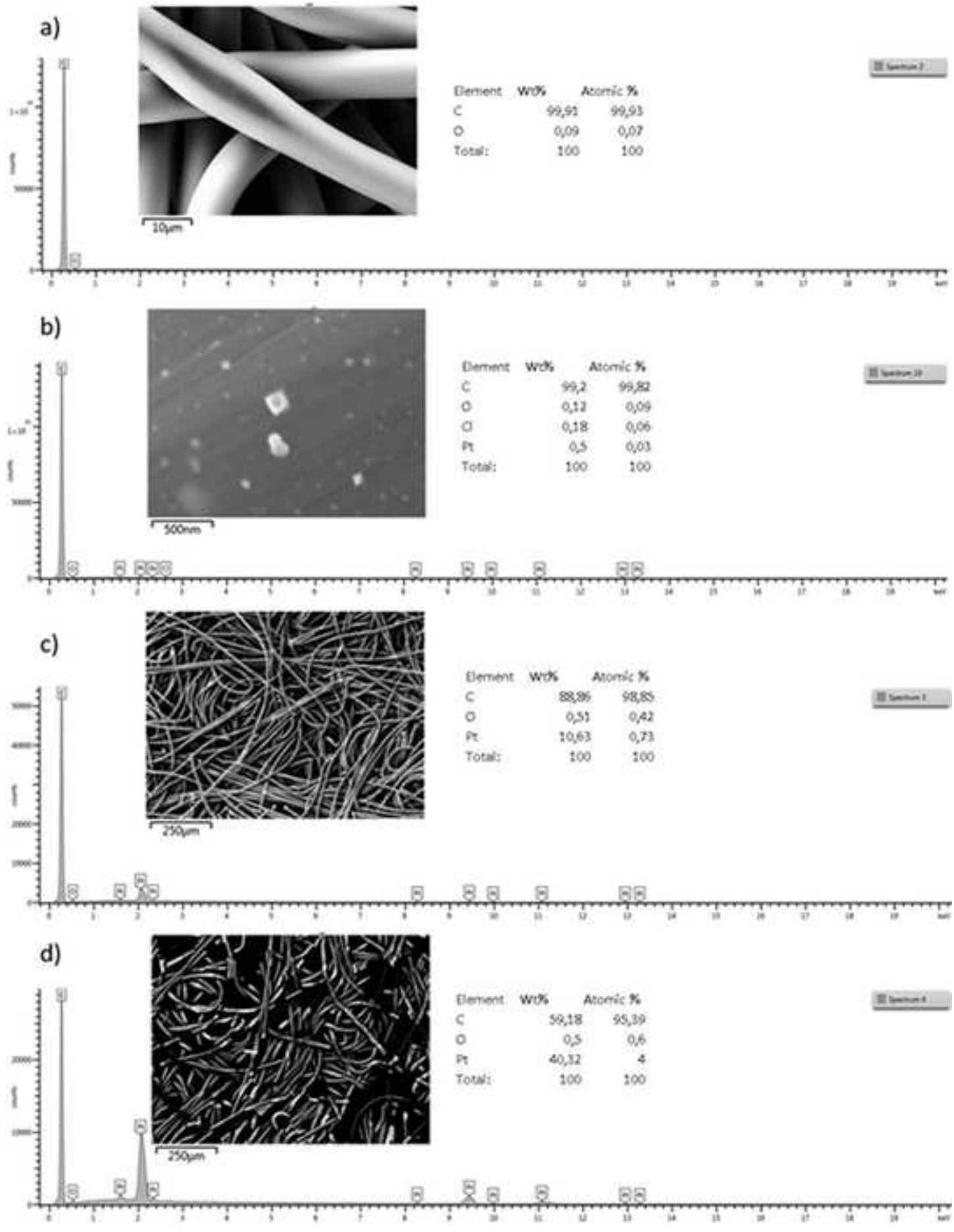

Figure 8

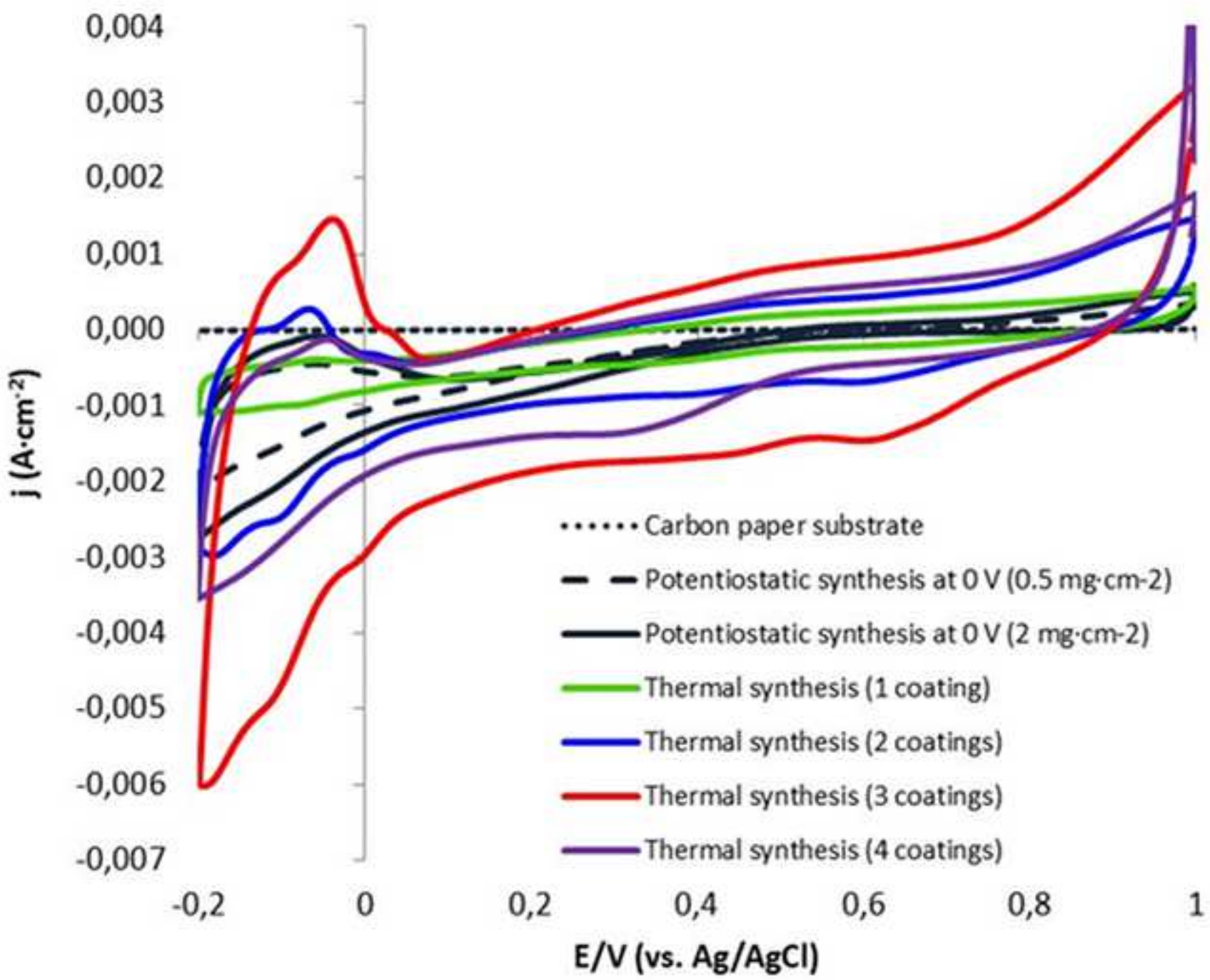

Figure 9

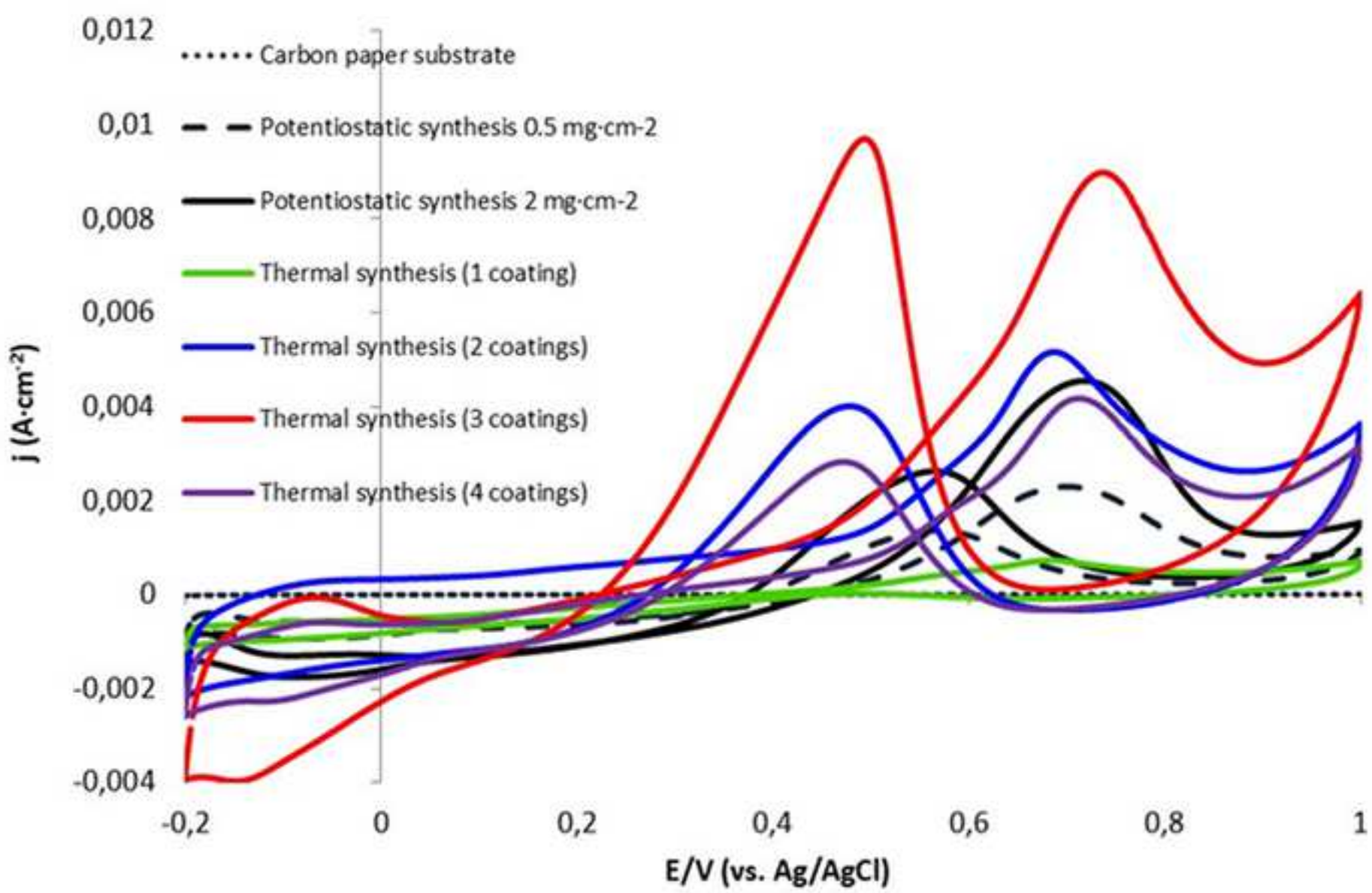

Figure 10

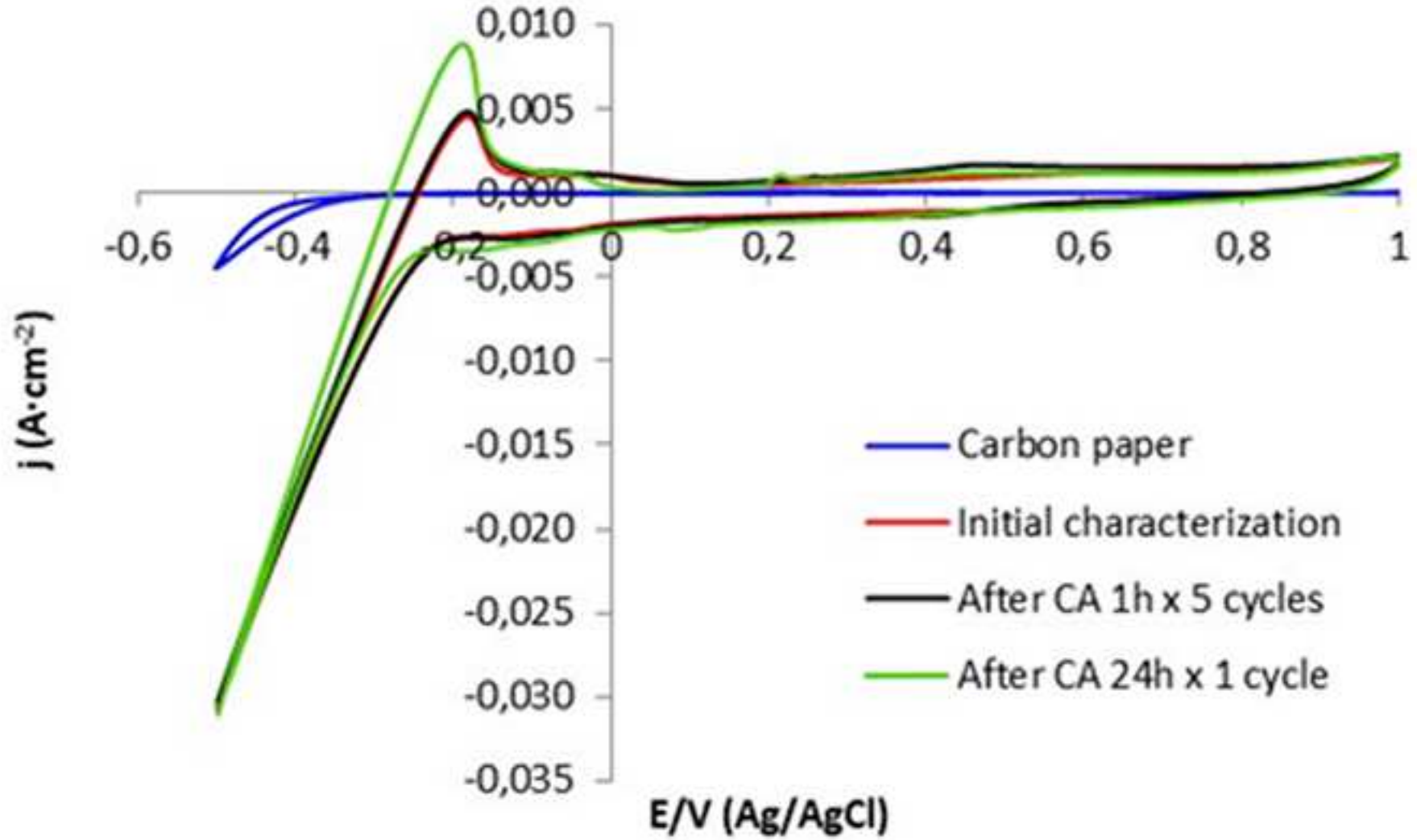

Figure 11

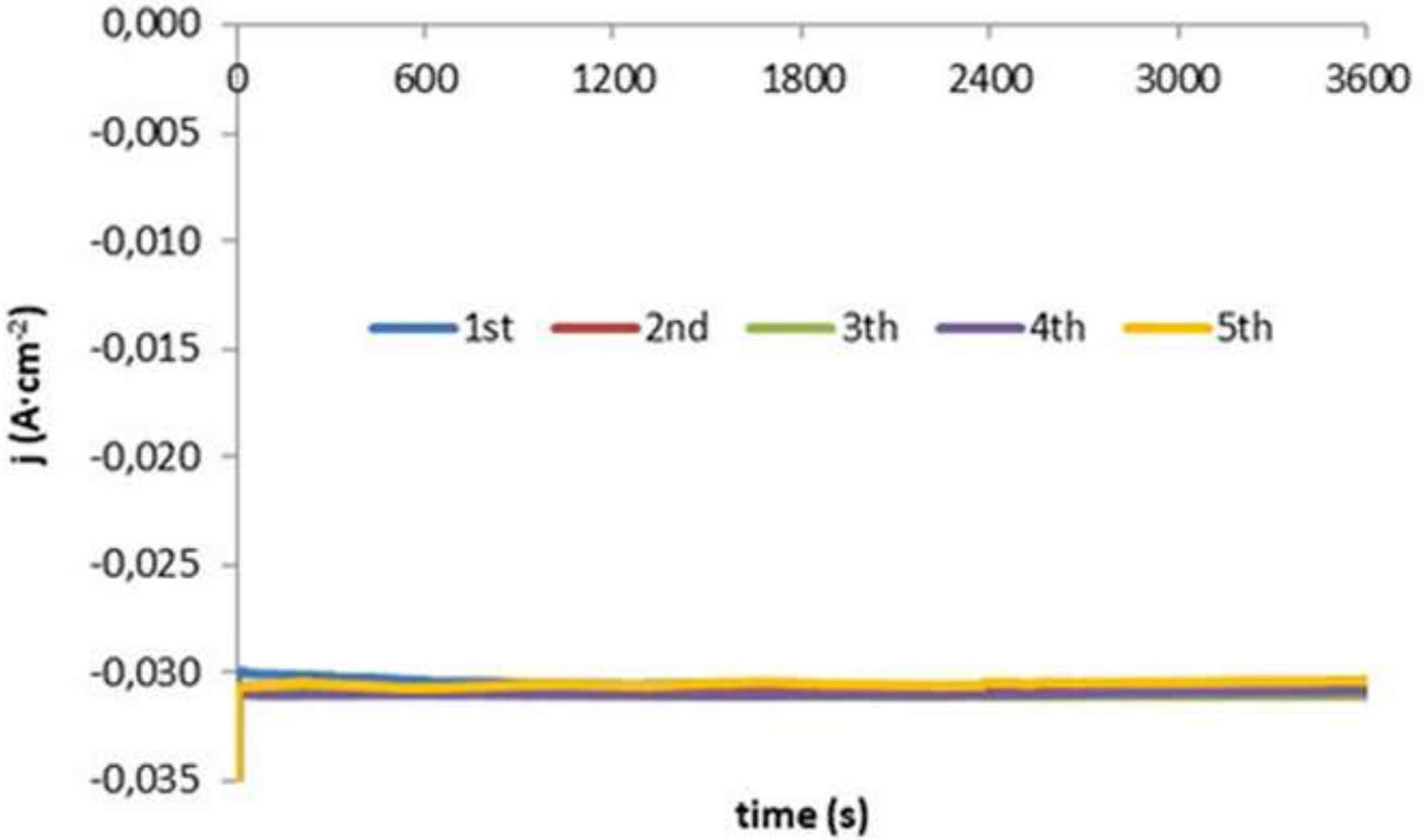

Figure 12